Environmental Science Processes & Impacts

ROYAL SOCIETY OF CHEMISTRY

PAPER

Published on 26 October 2026
Licensed under CC-BY 4.0

Check for updates

Cite this: DOI: 10.1039/d6em00205f

# Microplastics affect belowground performance of winter wheat and microbial networks in the rhizosphere

Katharina J. Neubert,*[a] Susanne Walch,[b] Michael Schloter[b] and Nicolas Brüggemann *[a]

Microplastics (MPs) are increasingly recognized as environmental pollutants affecting soil ecosystems and plant development, but their specific impacts on plant–soil–microbiome interactions remain unclear. This study investigated the effects of different MP types, including particulate polypropylene (PP), low-density polyethylene (LDPE), polystyrene (PS), and fibrous polyester (PES), individually on early-stage winter wheat root growth, nutrient concentrations, soil conditions and the rhizosphere microbiome using rhizotrons. Our findings revealed that PP and PES MPs significantly reduced root length. We observed increased soil ammonium concentrations with the addition of all MPs, likely due to reduced nitrifying bacterial activity, while PS MP enhanced soil nitrate concentration, potentially reflecting impaired root absorption. Because polymer size and morphology covaried, the results are interpreted as MP-type-specific. No significant effects of MPs on plant potassium (K) and phosphorus (P) uptake were observed. Despite changes in soil nutrient levels, we found no significant alterations in leaf growth, nutrient uptake, or chlorophyll content, indicating that root systems, though affected by MPs, remained sufficiently functional to support shoot development. Microbial co-occurrence analysis revealed two distinct microbial clusters in the rhizosphere, confirming modular microbial structure. Among all treatments, LDPE exposure induced the most pronounced increase in network complexity, as reflected by higher edge density, clustering coefficient, and natural connectivity compared to the control. Many amplicon sequence variants (ASVs), *e.g.*, members of Vicinamibacteraceae, *Pseudolabrys* and *Nitrospira japonica*, showed an increased degree and eigenvector centrality in the LDPE treatment, suggesting enhanced co-occurrence and higher influence within the microbial community structure. In contrast, the PES and PP treatments resulted in lower average node degree and reduced clustering. The PS treatment only had a small effect on the microbial co-occurrence networks. Overall, our data indicate that MP-induced stress can alter microbial network topology, reduce community integration, and drive shifts in ecologically important taxa in the rhizosphere, which are linked to changes in the availability of nutrients for plants. Our findings highlight the complex and variable influence of MPs on soil–plant interactions.

Received 16th March 2026
Accepted 25th October 2026

DOI: 10.1039/d6em00205f

rsc.li/espi

### Environmental significance

Microplastics are increasingly recognized as contaminants in agricultural soils, yet their impacts on plant–soil interactions remain poorly understood. This study demonstrates that microplastics can alter early winter wheat performance and rhizosphere microbial networks in polymer-specific ways. Fibrous and particulate microplastics disrupted microbial network structure, reduced root growth, and altered nitrogen cycling, including increased ammonium accumulation and shifts in nitrifying microbial taxa. In contrast, some polymers promoted more connected microbial communities without reducing plant growth. These findings highlight that microplastic pollution may influence crop productivity indirectly by restructuring soil microbial interactions and nutrient dynamics. Understanding polymer-specific effects is essential for predicting the environmental consequences of microplastics in agroecosystems and for developing sustainable soil management strategies.

## Introduction

The presence of microplastics (MPs), *i.e.*, plastic particles and fibers smaller than 5 mm, in soil has raised serious concerns due to their persistence and tendency to accumulate in agricultural systems. Agricultural soils, in particular, act as a major

[a]*Forschungszentrum Jülich GmbH, Institute of Bio- and Geosciences, Agrosphere (IBG-3), Wilhelm-Johnen-Straße, 52428 Jülich, Germany. E-mail: n.brueggemann@fz-juelich.de*

[b]*Research Unit for Comparative Microbiome Analysis (COMI), Helmholtz Munich, German Research Center for Environmental Health (GmbH), Neuherberg, Germany*

sink for MPs, with concentrations having increased markedly between 1966 and 2022.[1] The application of both organic (*e.g.*, farmyard manure and compost) and inorganic fertilizers further elevates MP loads in comparison to unamended soils.[2]

Although numerous studies have reported that MPs influence plant performance, the mechanisms underlying these effects remain poorly understood. Plants have been shown to respond to MP contamination with both growth inhibition and stimulation, depending on the context. For instance, some studies observed reduced biomass or nutrient uptake, whereas others found enhanced root and shoot development under specific conditions, such as drought.[3–5] However, the reasons for such divergent outcomes remain elusive because the processes linking MPs to plant responses occur through multiple, often interacting pathways within the soil environment, particularly in the rhizosphere.

From a physical perspective, MPs can modify soil structural and hydraulic properties, including porosity, aggregation, and water retention capacity, thereby influencing root penetration and water availability.[6–9] These structural changes can either hinder or facilitate plant growth, depending on soil texture, MP type, and environmental conditions.

From a chemical viewpoint, MPs have been reported to affect nutrient dynamics in the rhizosphere. For example, polyvinylchloride (PVC) particles may physically restrict root access to nutrients, leading to lower nitrogen (N) and phosphorus (P) uptake.[4] Conversely, improved aeration and nutrient mobility resulting from MP fiber incorporation have been linked to enhanced plant performance under drought stress.[3] These findings suggest that MPs can alter nutrient availability both directly and indirectly through changes in soil structure and chemistry.

Equally important are the biological effects of MPs on soil microbial communities, which play a central role in nutrient cycling and plant health. Strong MP-induced shifts in microbial diversity and community composition have been reported, including alterations in bacterial and fungal functional groups that may feedback on plant performance.[10–13] In addition, MP incorporation alters not only bacterial communities[10] but also fungal functional groups, such as pathogens, saprotrophs, and mutualists.[12] Recent syntheses indicate that many of the observed MP effects on plants likely stem from context-dependent processes in the rhizosphere – such as changes in microbial composition, enzyme activities, or symbiotic interactions – that are triggered or modulated by MPs.[14] Cross-ecosystem studies further show that MPs can alter microbial substrate use and that plastisphere communities undergo marked succession, although such findings do not directly demonstrate equivalent processes in agricultural rhizospheres.[15,16]

However, these fragmented approaches focusing either on chemical, physical or biological properties limit our ability to determine the dominant pathways through which MPs ultimately affect plant growth and health. To overcome this limitation and directly link an altered plant performance with MP-induced changes in soil chemistry, physics and biology in the rhizosphere, experimental systems are needed that allow plants to be grown under controlled conditions with direct observation of root development, while also enabling easy access to rhizosphere soil sampling. These requirements can be met with plant root observation chambers, called rhizotrons. Rhizotron experiments offer several advantages, such as (i) non-destructive *in situ* observation and monitoring of root growth and development over time, (ii) control of factors like soil moisture, nutrient availability, and compaction to study their effects on root growth, (iii) study of root-soil interactions, such as root penetration of different soil layers, rhizosphere processes, and the formation of root-soil mucilage complexes,[17] and (iv) validation of models where data obtained from rhizotron experiments can be used to validate and improve root growth and soil–plant–atmosphere continuum models, enhancing our understanding of root system functioning and its implications for crop productivity.[18] While rhizotrons have limitations in terms of scale and potential artifacts due to the narrow width of the growth compartment, they remain a valuable tool for studying root traits and processes that are difficult to observe under field conditions.

Current evidence shows that MP effects in soil–plant systems depend on interacting material and environmental attributes rather than polymer identity alone. We tested four common MP types: particles of low-density polyethylene (LDPE), polypropylene (PP), and polystyrene (PS), and polyester (PES) fibers. We used rhizotrons to assess root architecture, soil moisture and nutrient pools, bacterial community composition, and co-occurrence topology within one experiment. We hypothesized that the presence of MPs in the rhizosphere of wheat would: (i) reduce root growth, (ii) decrease nutrient availability through reduced root surface area, (iii) alter the rhizosphere microbiome, (iv) potentially mitigate the negative effects of MPs on shoot growth and vitality by changing the rhizosphere microbiome.

## Materials and methods

### Soil

The soil used for the experiment was a Luvisol with a loamy silt texture. The Luvisol was taken in June 2021 from a field at the agricultural research station Campus Klein-Altendorf of the University of Bonn, Germany (50.61 3614°N, 7.00 0713°E) from a depth of 0–20 cm. The soil was air-dried and sieved to 2 mm. The basic soil characteristics of the soil are listed in Table 1. The method for the determination of the volumetric water content at saturation is described in the SI.

### Microplastics

Based on results on MP pollution of German agricultural soils from the literature,[6,19] the following types of MP were considered significant for further investigation: particles of LDPE, PP, and PS, and PES fibers. LDPE, PP and PS were purchased from Goodfellow GmbH, Hamburg, Germany. While LDPE was obtained as powder with a particle size of 300–600 μm, PS and PP were ordered as 3–5 mm beads, which were shredded to powder with a conventional kitchen blender (BlendTec classic 575, Luba

 This journal is © The Royal Society of Chemistry 2026

Table 1 Characteristics of experimental soil[a]

| Soil type | Texture | Sand % | Silt % | Clay % | pH ($CaCl_2$) | $N_t$ % | $C_{org}$ % | $N_{min}$ μg $g^{-1}$ | $P_{av}$ μg $g^{-1}$ | $K_{av}$ μg $g^{-1}$ | VWC $cm^3$ $cm^{-3}$ |
|---|---|---|---|---|---|---|---|---|---|---|---|
| Luvisol | Loamy silt | 8 | 77 | 15 | 6.5 | 0.15 | 1.00 | 168 | 20 | 116 | 0.50 |

[a] With clay < 2 μm, silt 2–50 μm, sand 50–2000 μm, $CaCl_2$ = 0.01 M calcium chloride solution, $N_t$ = total nitrogen, $C_{org}$ = organic carbon, $N_{min}$ = plant-available mineral nitrogen, $P_{av}$ = available phosphorus, $K_{av}$ = available potassium, VWC = volumetric water content at saturation.

GmbH, Bad Homburg, Germany) and sieved to a particle size of 100–1000 μm with stainless steel analyzing sieves. The particle size distribution of all particle types is shown in Fig. S1. The PES fibers used were commercially available pillow filling material (JYSK Nordic A/S, Braband, Denmark) made from polyethylene terephthalate (Fig. S2) with a mean length of 28.8 ± 0.17 mm and a mean diameter of 0.74 ± 0.01 mm. All MPs were used as received and were not artificially weathered. The suppliers' documentation did not mention the addition of plasticizers or other additives.

### Experimental design

The rhizotrons had a size of 45 cm × 30 cm × 3.5 cm (height × length × width) and were covered with a transparent Plexiglas lid on one side, enabling root growth observation. Before filling the rhizotrons, air-dried Luvisol was mixed with the respective MP type at 0.4% w/w.[20,21] The control soil without addition of MP was processed in the same way. All rhizotrons were gradually filled with soil and stepwise compacted to reach a dry soil bulk density of 1.2 g $cm^{-3}$. Five replicates were prepared for each MP treatment and the control.

After the soil-filled rhizotrons had been watered and pre-incubated in a climate chamber at controlled conditions for one week (day/night, 16/8 h, $T$ = 22/10 °C; humidity = 60%), seeds of winter wheat (*Triticum aestivum* var. Nordkap, SAATEN-UNION GmbH, Isernhagen, Germany) were germinated in the dark at 10 °C on a moist paper towel for 24 h and then placed 2 cm deep into the soil in the center of each rhizotron. The plants were grown for 28 days, reaching principal growth stage 2 (tillering) according to the BBCH scale,[22] with 9 to 15 visible tillers. During the growth period, the rhizotrons' Plexiglas lids were covered with customized windshield covers for cars, and the rhizotrons were inclined by 45° to let roots grow in the dark close to the lids. While no fertilization of the soil was applied, the plants were allowed to grow under well-watered conditions. To compensate for soil water loss, rhizotrons were irrigated twice per week from above with irrigation water to maintain the soil water content at 25% w/w gravimetric water content (=60% gravimetric water-holding capacity, WHC), as determined by weighing the rhizotrons. In addition, shoot length was recorded over the course of growth period.

Soil samples were taken from each rhizotron before and after the growth period of 28 days. Since sampling required the opening of the lids, potentially destroying roots directly adhered to the lids, soil sampling during the growth period was avoided. Soil sampling was achieved by using stainless steel cylinders (10 cm × 1 cm length × diameter), inserted horizontally along the whole length of the root system. The soil samples were differentiated based on their proximity to the roots. The samples in direct contact with the roots were classified as rhizosphere soil, while the samples that were not in contact with the roots were classified as bulk soil. Soil and rhizosphere samples were stored at −20 °C for soil chemical and for microbiome analysis.

### Soil analysis

Two extractions were performed for each soil sample: (1) with 0.01 M $CaCl_2$ solution for plant-available mineral N content ($N_{min}$) analysis (VDLUFA, 2016), and (2) with calcium acetate/calcium lactate solution (CAL) for analysis of plant-available potassium ($K_{av}$) and plant-available phosphate ($P_{av}$) based on VDLUFA (2016). The respective pH values of soil samples were measured in the 0.01 M $CaCl_2$ extracts for 5 min each with a pH meter (Multi 3630 IDS, Xylem Analytics Germany GmbH, Weilheim, Germany). The method for the determination of the volumetric water content at saturation as well as a detailed description of the above-mentioned methods is described in the SI.

### Root analysis *via* WinRHIZO

Root systems, together with the surrounding soil, were removed from the rhizotrons and placed in plastic bags until further processing. Root fragmentation during transfer was considered negligible, as root length was determined by scanning root images using a flatbed scanner (Epson Perfection LA2400, Epson Deutschland GmbH, Düsseldorf, Germany) and the WinRHIZO image analyzing system (Regent Instruments Inc., Québec, Canada), quantifying individual fragments, which were summed up to total root length. All root fragments were washed from the soil with a shower head over a 2-mm sieve. Finally, roots were collected from the sieve and were stored in 50% v/v ethanol/water until roots were scanned and analyzed. A batch analysis of all scans was accomplished with the parameters defined in Table S2. The diameter range of harvested roots was determined from stereomicroscopic images (Fig. S3), ranging from 0–0.4 mm for lateral roots, and from 0.4–1 mm for primary roots. Total root surface area was used to calculate soil nutrient content per root surface area (RSA).

### Leaf pigment analysis

Leaf pigments from 28-days-old winter wheat shoots were analyzed as described by Lichtenthaler & Wellburn (1983).[23] Briefly, portions of 20 mg of dried (at 60 °C, 7 d) and ball-milled (MM200, Retsch GmbH, Haan, Germany) winter wheat leaves

were weighed into 5-ml Eppendorf vials in triplicate and mixed with 5 ml of an acetone–water mixture (4 : 1 v/v) (acetone: analysis grade ≥99.8%, Honeywell International, Inc., Offenbach, Germany). Vials were vortexed for 5 s and shaken for 90 min at 200 rpm in the dark, before they were centrifuged at 1823×*g* (2800 rpm) for 15 min. Each of the supernatants (2 ml) were transferred into cuvettes and measured photometrically (Genesys 50, Thermo Fisher Scientific, Darmstadt, Germany) at 470, 646 and 663 nm against a blank of the prepared extraction medium. Equations to calculate the amount of chlorophyll *a* ($chl_a$), chlorophyll *b* ($chl_b$) and the carotenoid (car) content of the extracts are shown in the SI.

### Statistical analysis of the soil and plant data

All plant growth, soil nutrient, and leaf characteristics were analyzed using a two-way ANOVA with treatment and soil compartment as fixed factors, including the treatment × soil compartment interaction. The data were tested for normal distribution with the Kolmogorov–Smirnov test. Residuals and homogeneity of variance were assessed using residual diagnostics and the Brown–Forsythe test. Because variances were homogeneous, simple-effect comparisons between each treatment and the control within each soil compartment were performed using a homoscedastic one-sided *t*-test. *P*-values for multiple comparisons were adjusted using the Holm–Bonferroni procedure.

### Microbiome analysis

**DNA extraction and library preparation.** Genomic DNA was extracted from frozen rhizosphere soil using the NucleoSpin® Soil Kit (Macherey-Nagel, Düren, Germany) with SL1 buffer for lysis. An extraction without soil was included as negative control. DNA quantity was measured using the Quant-iT PicoGreen dsDNA Assay Kit (Thermo Fisher Scientific, Darmstadt, Germany). Bacterial communities were assessed following the 16S Metagenomics Sequencing Library Preparation protocol (Illumina, San Diego, CA, USA) and quality guidelines.[24] The v4 region of the 16S rRNA gene was amplified using primers 515F and 806R in 25 µl reactions containing 10 ng DNA, 0.5 µl of each primer (10 pmol), 2.5 µl 3% BSA, 12.5 µl NEBNext High-Fidelity 2× PCR MasterMix (New England Biolabs, Frankfurt am Main, Germany), and DEPC-treated water. Products were purified using MagSi NGSprep Plus beads (Steinbrenner, Germany) and quantified with a Fragment Analyzer 5200 (Agilent Technologies, Santa Clara, CA, USA) using the NGS Fragment Kit (1–6000 bp). Indexing PCR (25 µl) contained 10 ng purified amplicon, 2.5 µl of each indexing primer (Nextera® XT Index Kit v2 Set C or D; Illumina, San Diego, CA, USA), 12.5 µl NEBNext High-Fidelity 2× PCR MasterMix, and 6.5 µl DEPC-treated water. Indexed amplicons were purified, quantified, diluted to 4 nM, pooled equimolarly, and sequenced paired-end on a MiSeq® usinq the MiSeq® Reagent kit v3 (600 cycles).

**Processing and statistical analysis of the sequencing data.** Sequences were processed on Galaxy.[25] Reads were trimmed to ≥50 bp with Cutadapt,[26] quality checked with FastQC,[27] and denoised with DADA2 (Galaxy Version 1.30.0)[28] using: trim = 20 bp from 5′ end, truncLen = 240/200 (F/R), max EE = 3/4. Taxonomy was assigned using SILVA v138.1 (99%).[29] Amplicon sequence variants (ASVs) present in controls, unassigned, mitochondrial, chloroplast, or singleton reads were removed. The raw sequence data obtained in this study are deposited in the short-read archive of NCBI under accession number PRJNA1422079. Analyses were conducted in R 4.3.1.[30]

Alpha diversity was calculated using species richness based on ASV number. To further characterize differences in microbial community composition, the beta diversity was analyzed *via* unweighted and weighted UniFrac distance matrix. Bray–Curtis dissimilarities were calculated from total-sum-scaled (TSS)- normalized ASV abundances, while binary Jaccard distances were used to assess differences in ASV presence and absence. In addition, Aitchison distances were calculated from centered log-ratio (CLR)-transformed ASV data to account for the compositional nature of the sequencing data.

Differences in community composition between groups were evaluated using PERMANOVA. *P*-values were adjusted for multiple comparisons using the Benjamini–Hochberg procedure. Differentially abundant taxa were identified using ANCOM-BC2, with global and pairwise comparisons performed between groups. Benjamini–Hochberg-adjusted *p*-values were used to determine statistical significance ($p < 0.05$). For taxa showing significant global differential abundance, log-fold changes (LFC) from the pairwise comparisons were visualized as a heatmap. Significance groupings were represented by letters, with groups sharing the same letter indicating no significant difference between them.

Plots were created in R using ggplot2, ggpubr and metacoder. Venn diagrams for core microbiome analysis were made using Venny[31] with a minimum ASV threshold of 75% (ASV must be present in 75% of the samples to be considered for the group). Microbial co-occurrence networks were inferred using Pearson correlations in NetCoMi v1.1.0,[32] retaining ASVs present in ≥4/5 replicates per treatment (control: 1628 ASVs, LDPE: 1544 ASVs, PES: 1596 ASVs, PP: 1852 ASVs, PS: 1582 ASVs). Data were clr-transformed, zeros replaced *via* "multRepl", sparsified at 0.3 threshold, and converted to dissimilarities using the "signed" method. Network modules were identified with the cluster_fast_greedy algorithm. Visualizations were limited to the top 100 ASVs. To relate microbial community composition to plant function, the metadata were merged and analyzed in R using the packages phyloseq, vegan, tidyverse and ggplot2. An environmental fitting analysis (envfit) was applied to test the correlation between microbiome and plant-available nutrients. Significant variables ($p < 0.05$) were visualized as scaled vectors in a PCoA biplot.

## Results

### Root and shoot analysis

The roots harvested from the individual rhizotrons ranged between 1200 and 1700 cm total length (Fig. 1). Lateral roots accounted for 87% to 92% of total length. Root growth significantly decreased by 31% ± 20% ($p = 0.02$) in PP-amended soil. Soil mixed with PES fibers resulted in a weakly significant

 This journal is © The Royal Society of Chemistry 2026

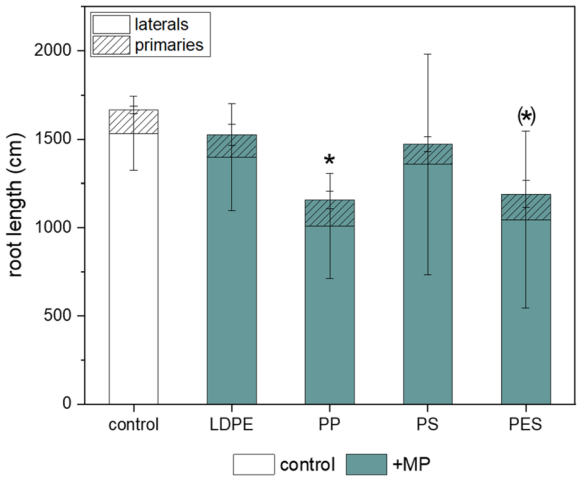


Fig. 1 Root length of winter wheat plants grown in rhizotrons for 28 days. "+MP" indicates MP addition to soil, while no MP was added to control. The following MP types were added: LDPE = low-density polyethylene, PP = polypropylene, PS = polystyrene, PES = polyester fibers. Hatched areas of the bars represent the portion of primary roots (0.4–1 mm in width), and unhatched areas the portion of lateral roots (0–0.4 mm in width). Whiskers represent the standard deviation of five replicates. The asterisk indicates significant difference ($p \leq 0.05$), while the asterisk in parentheses shows a weakly significant difference ($0.05 \leq p \leq 0.1$) to the control, which was tested with a one-sided, homoscedastic *t*-test.

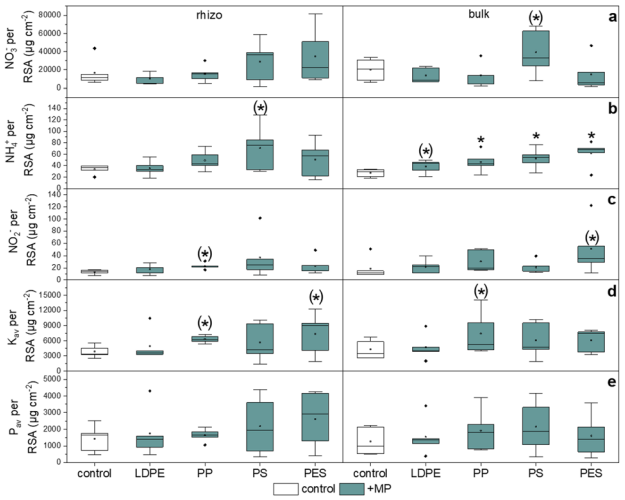


Fig. 2 Plant-available nutrients per root surface area (RSA) (in μg $cm^{-2}$) of (a) nitrate ($NO_3^-$), (b) ammonium ($NH_4^+$), (c) nitrite ($NO_2^-$), (d) potassium ($K_{av}$) and (e) phosphate ($P_{av}$) in rhizosphere (rhizo) and bulk soil after winter wheat was grown for 28 days in rhizotrons. "+MP" indicates MP addition to soil, while the control represents soil without MP addition. The following MP types were added to the soil: LDPE = low-density polyethylene particles, PP = polypropylene particles, PS = polystyrene particles, PES = polyester fibers. Boxes are the interquartile range (IQR) from the 25th to 75th percentile, lines inside boxes indicate the median, white squares indicate the mean values, upper and lower whiskers are 1.5 times the IQR and diamond-shaped markers are outliers ($n = 5$). Asterisks show significant differences ($p \leq 0.05$) and asterisks in parentheses show weakly significant differences ($0.05 \leq p \leq 0.1$) to the control, tested with one-sided, homoscedastic *t*-test.

reduction in root growth of 29% ± 35% ($p = 0.09$) compared to the control.

Gravimetric (Fig. S4a) and length measurements of shoots (Fig. S4b), nitrogen content in leaves (Fig. S4c and S4d), leaf pigment analysis (Fig. S5), and shoot growth over time (Fig. S6) showed no significant differences between +MP treatments and the control.

## Soil nutrient analysis

**Root surface area-based soil nutrient availability.** Soil nutrient concentrations, *i.e.*, nitrate ($NO_3^-$), nitrite ($NO_2^-$), ammonium ($NH_4^+$), $K_{av}$, and $P_{av}$, on a weight basis (in μg $g^{-1}$) are shown in Fig. S7. They were used to calculate plant-available nutrients per RSA (Fig. 2). This provided a clearer picture of nutrient availability to individual root systems, which varied in length and surface area between different treatments and replicates.

For $NO_3^-$ per RSA, only soil containing PS particles showed a weakly significant increase compared to the control (+96% ±110%, $p = 0.09$). The $NH_4^+$ per RSA in bulk soil was significantly higher in the presence of PP (+71%, $p = 0.04$), PS particles (+93%, $p = 0.02$), and PES fibers (+126%, $p = 0.01$), with a weakly significant increase observed in soil containing LDPE particles (+42%, $p = 0.05$). In the rhizosphere soil, $NH_4^+$ per RSA was weakly significantly enhanced in the presence of PS particles (+111%, $p = 0.06$). The $NO_2^-$ per RSA showed a weakly significant increase with PP particles in the rhizosphere soil (+101%, $p = 0.1$) and with PES fibers in the bulk soil (+167%, $p = 0.09$). Additionally, $K_{av}$ per RSA increased in both rhizosphere and bulk soil with PP particles by 98% ($p = 0.09$) and 74% ($p = 0.09$), respectively, and in the rhizosphere soil with PES fibers (+91%, $p = 0.07$). The $P_{av}$ amount per RSA showed no significant difference between the treatments and the control.

**Statistical evaluation of soil nutrient availability and root uptake.** A two-way ANOVA was conducted to examine the effects of the root zone (rhizosphere soil) and the type of MP on soil nutrient availability for roots (Table S3). Significant effects of MPs were found for $NO_3^-$ and $NH_4^+$ per RSA. In contrast, there were no significant effects of soil compartment or soil compartment × MP interaction. The type of MP affected the amount of $NO_3^-$ per RSA, with an effect size of 20% ($F(4,40) = 2.76$, $p = 0.04$). The highest amount of $NO_3^-$ per RSA in soil was observed for the treatment with PS particles (39 mg $cm^{-2}$), while for all other MPs (LDPE, PP and PES) the soil $NO_3^-$ availability was not significantly different from the control.

$NH_4^+$ availability was significantly affected by MP addition ($F(4,40) = 3.65$, $p = 0.01$). In the control, the rhizosphere soil had 23% more $NH_4^+$ per RSA compared to the bulk soil. Significantly enhanced $NH_4^+$ concentrations (42–126%) were measured in the bulk soil of all MP treatments compared to the control.

Plotting $K_{av}$ *versus* $P_{av}$ revealed a high correlation for the +MP treatments ($R^2 = 0.77$) and for the control ($R^2 = 0.83$) (Fig. 3). These high correlations suggest simultaneous root uptake of both nutrients ($P_{av}$ and $K_{av}$). The linear fit for the +MP

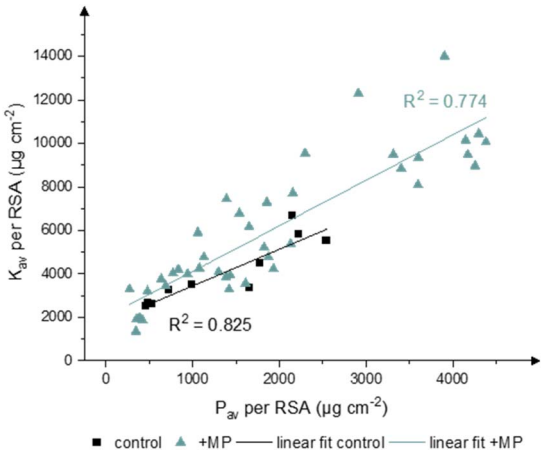


Fig. 3 Plant-available potassium ($K_{av}$) *versus* plant-available phosphate ($P_{av}$) content per root surface area (RSA) (in µg cm$^{-2}$) in MP-amended soil (+MP, green triangles) and the control (black squares) without MP after winter wheat was grown for 28 days in the rhizotrons.

treatments had a steeper slope compared to the control, indicating higher nutrient availability per RSA and presumably less uptake of $P_{av}$ and $K_{av}$. In contrast, the plot of $NO_2^-$ *versus* $NH_4^+$ showed weak correlations for both +MP ($R^2 = 0.43$) and the control ($R^2 = 0.05$) (Fig. S8), as well as the plot of $NO_3^-$ *vs.* $NH_4^+$ (for +MP: $R^2 = 0.08$, and for control: $R^2 = 0.54$) (Fig. S9), indicating only a weak relationship between these parameters. Soil nutrient analysis also revealed a significant increase in $NH_4^+$ in the bulk soil of +PP, +PS, and +PES (Fig. 2b), coinciding with a low correlation between $NH_4^+$ and $NO_2^-$.

## Microbiome analysis

**Sequencing quality and diversity analysis.** After denoising, 13 634 664 reads were processed, of which 13 133 646 were left after quality filtering (removal of singletons and unassigned ASVs) and removal of ASVs detected in the extraction or PCR control sample. Sequencing of the generated amplicons resulted in 44 905 to 143 559 reads per sample after quality filtering. To compare samples without statistical bias, a subsampling strategy of 44 905 reads per sample was performed, reflecting the lowest observed read number. In total, 15 853 ASVs were detected. 108 ASVs present in the non-template control were excluded from the dataset. Rarefaction analysis indicated that the resulting sampling depth was sufficient for further analysis of all samples (Fig. S13). Alpha diversity analysis revealed no significant differences between bulk soil and rhizosphere samples ($p = 0.652$), nor between the different MP treatments ($p = 0.721$) (Fig. 4 and Table S4).

The Bray–Curtis analysis showed no significant effect of MP treatment ($R^2 = 0.159$, $p = 0.349$), soil compartment ($R^2 = 0.0065$, $p = 0.277$), or the MP-soil interaction ($R^2 = 0.018$, $p = 0.193$). Additionally, no significant effects were detected using Jaccard distances or Aitchison distances (Fig. S11). None of the applied beta-diversity measures provided evidence for a significant shift in overall microbial community composition associated with MP treatment, soil compartment, or their interaction.

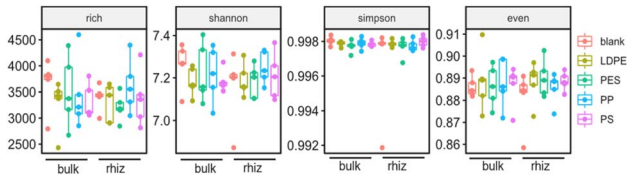


Fig. 4 Alpha-diversity indices of the bacterial community structure in bulk soil (bulk) and rhizosphere soil (rhizo). Rich = observed richness, shannon = shannon index, simpson = simpson index, even = Pielou's evenness.

To complement the diversity analyses, a differential-abundance analysis was performed using the compositionality-aware method ANCOM-BC2. A global ANCOM-BC2 test was first used to identify candidate ASVs showing evidence of differential abundance across MP treatment, using an unadjusted $p < 0.05$ as the candidate-selection threshold. Pairwise comparison between MP treatments were subsequently performed for these candidate ASVs. The resulting pairwise differential-abundance patterns are shown in Fig. S12. No significant differential-abundance patterns were detected.

**Comparative analysis of major ASVs across treatments.** For the core microbiome analysis, all ASVs with at least 0.1% reads in 75% of the samples per group were considered. This revealed 92 ASVs in total, with 50 ASVs shared by all groups, representing the core microbiome (Fig. 5). Core ASVs primarily belong to the phyla *Crenarchaeota*, *Actinobacteria*, *Acidobacteria*, and *Proteobacteria*. Twenty-seven ASVs were exclusively detected in MP-treated samples, *e.g.* ASVs typical for *Lysobacter* and *Sphingomonas*. Unique ASVs were detected for PES, PP, and PS. Two ASVs of RB41 (*Acidobacteriota*), an unclassified member of *Vicinamibacterales*, Ellin6067 (*Proteobacteria*), and an unclassified ASV of KD4-96 (*Chloroflexi*) were detected exclusively in PES-treated samples, whereas *Chryseolinea* was detected exclusively in PP-treated samples, and a member of *Thermomonas* in PS-treated samples. Three ASVs identified as *Acidibacter*, *Intrasporangiaceae*, and *Vicinamibacteraceae* were only found in MP-free samples. Some ASVs were specific for certain MP

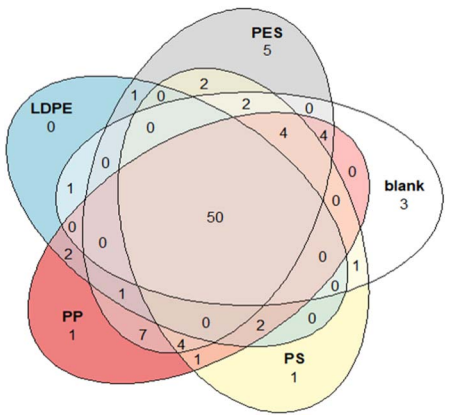


Fig. 5 Venn diagram of shared ASVs between MP materials and MP-treated soil and rhizosphere. All ASVs with at least 0.1% reads in 75% of the samples per group were considered for core microbiome analysis.

 This journal is © The Royal Society of Chemistry 2026

materials. For example, seven ASVs were only detected in PES- and PP-treated samples, namely *Pseudolabrys*, *Gemmatimonas*, and two unclassified ASVs of *Vicinamibacterales* (*Acidobacteriota*), one of Subgroup 10 (*Acidobacteriota*), one of *Comamonadaceae* (*Proteobacteria*), and one of *Nitrososphaeraceae*. PS- and PES-treated samples shared exclusively two ASVs assigned to *Sphingomonas*. PP- and PS-treated samples shared an unclassified ASV of DS-100 (*Acidobacteriota*). In contrast, PS- and LDPE-treated samples did not share any unique ASVs.

**Effects of different MP types on microbial co-occurrence networks in the rhizosphere.** Microbial co-occurrence networks in the rhizosphere were constructed to assess how different MP types influenced microbial community structure and interactions (Fig. 6). Across treatments, rhizosphere networks consisted of 86–88 nodes, representing ASVs, and were characterized by high overall connectivity and a stable ratio of positive associations (~49%), indicating generally cohesive microbial communities under all conditions. However, distinct polymers induced specific structural shifts in network topology, centrality, and robustness.

Exposure to LDPE slightly increased overall network complexity and connectivity compared to the control. The LDPE network showed higher average node degree, eigenvector and closeness centrality, and clustering coefficients, suggesting strengthened microbial associations and greater network integration. Candidate central ASVs, such as *Vicinamibacteraceae* (ASV01049), *Pseudolabrys* (ASV11937), and *Nitrospira japonica* (ASV08768), exhibited increased centrality, indicating enhanced ecological importance in the LDPE treatment. Although natural connectivity was marginally higher in the LDPE treatment, implying greater robustness to random loss, vertex connectivity was lower, suggesting reduced resistance to fragmentation.

In contrast, PES exposure reduced overall network connectivity and resilience. The PES network showed lower average node degree, closeness, and eigenvector centrality than the control, but higher betweenness centrality, indicating a more fragmented and reorganized structure. Local clustering and edge density decreased, and both natural and vertex connectivity declined, reflecting diminished structural robustness. Network-central ASVs, such as *Vicinamibacterales* (ASV01002), *Oryzihumus terrae* (ASV01604), and *Thermomonas* (ASV13638), retained central positions but their influence weakened in the presence of PES, pointing to reduced network cohesion and stability.

Similarly, the PP treatment resulted in moderate declines in connectivity and centrality relative to the control. The PP network exhibited lower node degree, eigenvector centrality, clustering, and natural connectivity, accompanied by a small reduction in edge density. While the influence of major

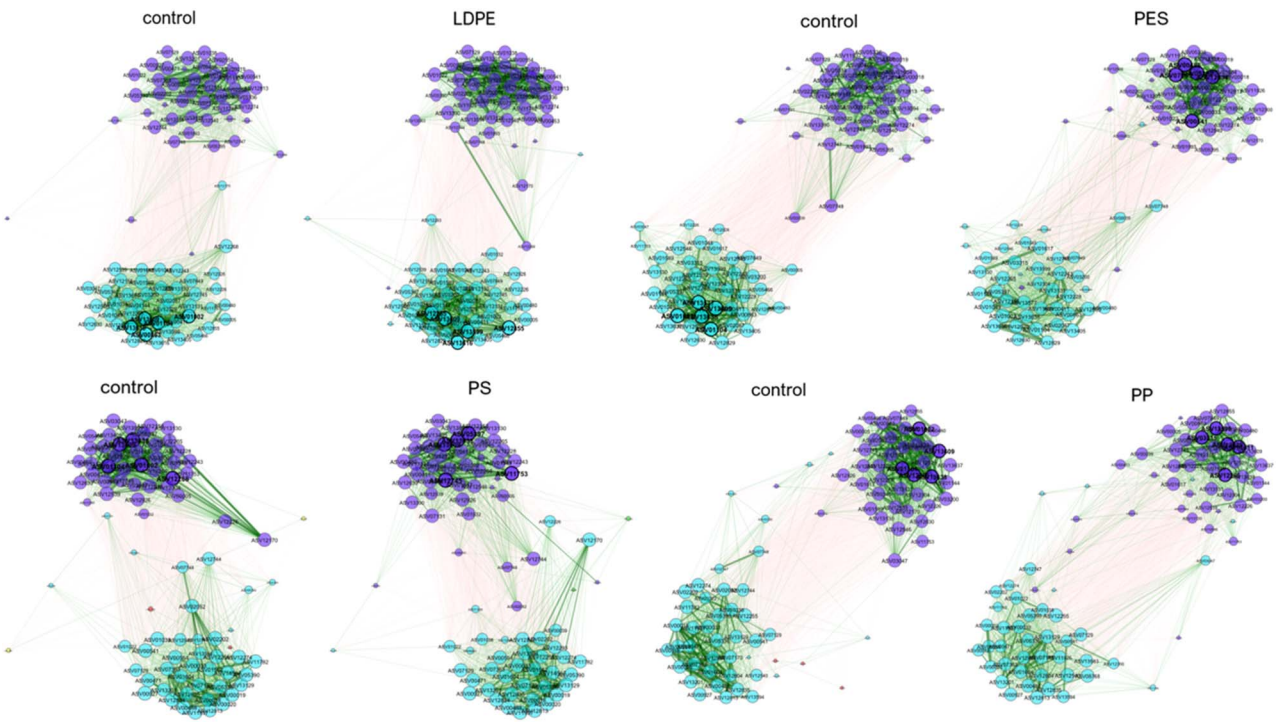


Fig. 6 Microbial co-occurrence networks based on Pearson correlations for untreated (control) and MP-treated (LDPE, PES, PS, PP) rhizosphere samples. Each node represents an amplicon sequence variant (ASV), with node size proportional to its degree (number of connections). Node colors (purple and turquoise) indicate network modules (communities) identified by correlation-based clustering, representing groups of ASVs that are more strongly co-occurring with each other. All networks are compartmentalized, consisting of two hubs of microbial taxa that frequently interact and/or respond similarly to environmental cues. Edges represent significant correlations between ASVs (green = positive; red = negative). The networks include core ASVs, defined as those present in at least four out of five replicates. Displayed are the 100 most abundant ASVs.

network-central taxa (*Vicinamibacterales*, *Oryzihumus terrae*, *Thermomonas*) decreased, new taxa such as JGI 0001001-H03 (ASV00384) and mle 1-27 (ASV08274) gained importance through higher betweenness centrality, indicating a redistribution of structural roles within the network.

The PS network remained fully connected and comparable in size and density to its control, yet showed subtle shifts in node-level properties. Network-central taxa such as *Candidatus* Nitrosocosmicus (ASV00005), *Blastocellaceae* (ASV00411), and *Vicinamibacterales* (ASV01002) decreased in centrality, while *Thermomonas* (ASV13638) and *Nitrospira japonica* (ASV08768) gained influence. Clustering and natural connectivity declined slightly, whereas vertex connectivity increased marginally, indicating minor structural reorganization but preserved overall network integrity.

**Combined effects of the different MPs on microbiome and soil nutrients.** A principal coordinate analysis (PCoA) based on the microbiome and plant performance data (normalized root surface area), coupled with an *envfit* analysis, identified three plant nutrients that were significantly linked to shifts in microbial community structure (Fig. 7), including $NH_4^+$ ($p = 0.0451$), $NO_2^-$ ($p = 0.0111$), and $P_{av}$ ($p = 0.0008$). The direction and length of the vectors represent the gradient and strength of the association between nutrient concentrations and community dissimilarity in the ordination space. In the ordination space, PS- and PP-treated samples were positioned in the direction of $NO_2^-$ and $NH_4^+$ vectors, showing that variation in community composition along the PCoA axes was associated with increasing concentrations of those nitrogen forms. In contrast, the $P_{av}$ vector pointed in the opposite direction, suggesting that microbial communities in the control and, to a lower extent, in the PES treatment were associated with higher phosphate availability.

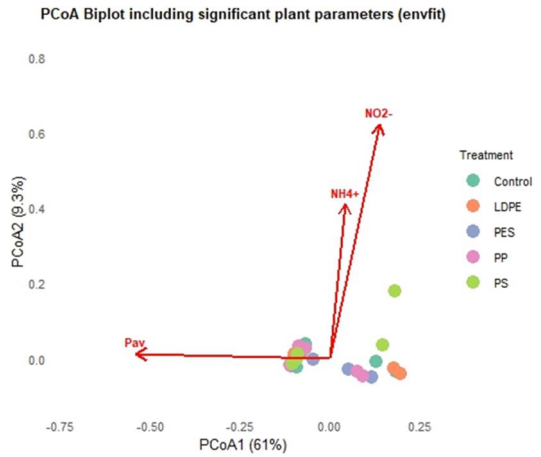


Fig. 7 Principal coordinate analysis (PCoA) of rhizosphere bacterial community composition associated with winter wheat after 28 days of growth, exposed to different MP treatments (control, LDPE, PES, PP, PS). The ordination is based on Bray–Curtis dissimilarities of the microbial community composition. Red arrows indicate significant ($p < 0.05$) plant-available nutrient parameters fitted by *envfit*, showing correlations with community structure: plant-available ammonium ($NH_4^+$), nitrite ($NO_2^-$), and phosphate ($P_{av}$). The direction and length of the arrows show the gradient and strength of the correlation, respectively. The plot illustrates that variations in microbial communities are partly explained by the availability of plant nutrients in the rhizosphere.

# Discussion

Our results demonstrated that MP effects on early winter wheat performance were strongly polymer-type and shape-specific, and closely linked to shifts in rhizosphere microbial network structure and function. Our experiment was designed to enable comparison among the four MP types tested, but it did not factorially separate polymer chemistry, particle size, morphology, or surface aging. Because LDPE, PP, PS, and PES differed simultaneously in polymer size, distribution and geometry, these contrasts could not be attributed to polymer chemistry alone. In addition, only one MP concentration was tested, hence the experiment was not designed to establish a dose-response relationship. The study consequently evaluated integrated MP-type responses rather than isolated polymer mechanisms.

### Microplastic type-driven alterations in root development, microbial networks, and nutrient cycling

Among the tested MPs, PP particles and PES fibers consistently reduced root length, with effects comparable to those reported in previous studies. For instance, PP MPs at a concentration of 0.1% w/w have been shown to impair root growth, germination, and biomass, while also modifying soil enzyme activities – such as reduced phytase and increased dehydrogenase activity – and disrupting rhizosphere bacterial connections (*i.e.*, nutrient exchange, signaling, cooperative metabolism).[33] Similarly, PES fibers at 0.5% w/w in soil have been reported to reduce both root length and biomass (−30%) in maize after 34 days.[7,8] This reduction in root length suggests that the presence of PES fibers in the soil adversely affects root development, which can have implications for overall plant health and nutrient uptake. Unlike our results, these studies also highlighted detrimental effects on both shoot and root biomass, indicating that MP effects vary across plant and soil types.[7,8]

In our study, the negative impacts of PP and PES on root development coincided with fragmentation of the microbial co-occurrence network in the PES treatment, indicated by lower node degree, clustering coefficients, eigenvector and closeness centrality. This network simplification points to weakened microbial cooperation and reduced functional integration, which can limit plant-beneficial services such as nutrient mineralization, phytohormone production, and pathogen suppression.[34,35] However, this finding should not be interpreted as evidence that microbial network fragmentation caused reduced root growth. Both patterns may instead reflect shared responses to altered soil physical or chemical conditions.

Responses on nutrient turnover processes further support this link. Across all MP treatments, bulk soil $NH_4^+$ concentrations increased significantly (Fig. 2b), with the largest effect

 This journal is © The Royal Society of Chemistry 2026

sizes observed for PP and PES ($\eta^2 = 25\%$; Table S3). A similar $NH_4^+$ accumulation has been reported previously for PP MP pollution.[36] The accumulation of $NH_4^+$, particularly in the PP and PES treatments, may be associated with microbial network fragmentation, lower edge density, and the reduced influence of formerly central taxa such as *Thermomonas* and *Sphingomonas*. However, the single end-point sampling design provides no temporal evidence that microbial network changes preceded changes in $NH_4^+$.

MPs can also create novel microbial habitats,[11] potentially altering nutrient cycling. However, since our study did not include direct measurements of nitrification and denitrification rates, microbial functional genes, or enzyme activities, the underlying mechanisms remain uncertain, and we can only infer potential explanations from the observed microbial network patterns. Higher $NH_4^+$ pools may be attributed to reduced microbial nitrification activity (*e.g.*, inhibition of nitrifying bacteria),[37] but other possible explanations include increased mineralization of organic matter (*i.e.*, ammonification), decreased nutrient uptake by roots and/or microbes, and altered solute transport.

Soil $NO_3^-$ dynamics were more MP-specific. The ANOVA showed a large effect of MP type on soil $NO_3^-$ concentration ($\eta^2 = 20\%$, Table S3). PS particles increased $NO_3^-$ availability per RSA, while LDPE, PP, and PES had no significant effect. Elevated $NO_3^-$ levels can arise from reduced plant uptake, increased nitrification, reduced denitrification, or decreased microbial uptake. For example, Rillig *et al.* (2021) found that MP fibers at 0.4% w/w altered N mineralization and nitrification,[38] increasing $NO_3^-$ due to enhanced soil aeration, which stimulated nitrification and inhibited denitrification. Similarly, de Souza Machado *et al.* (2019) reported that PS particles (at 2% w/w) altered soil structure in ways that could indirectly affect nutrient availability.[39] In our study, PS-treated soils showed increased influence of nitrifying taxa such as *Nitrospira japonica*,[40] suggesting functional reorganization. However, although *Nitrospira japonica* was in a more central position in the PS correlation network, this does not indicate greater abundance, activity, or nitrification rate.

The relationships between other nutrients were less affected by MP type. However, we found a significant correlation between soil $P_{av}$ and $K_{av}$ concentrations, which is consistent with previous studies showing that wheat roots take up these nutrients simultaneously.[41–43] This relationship was either not or similarly affected by MP addition across treatments. Reports in the literature on the effects of MPs on K dynamics vary. For example, PE MPs at 0.5% w/w reduced K leaching,[44] but plastic film mulching had no effect on soil K content.[45] Similarly, we did not see any MP effect on soil K content in our study.

MP effects on soil pH also varied in previous studies. Zhao *et al.* (2021) observed pH fluctuations over time after MP addition (initial increase, then decrease, then increase again),[46] while Yin *et al.* (2007) found no effect of PP groundcover sheets on soil pH. Our findings of no significant pH change are in line with the latter study.[47]

Soil water dynamics showed MP-type dependent responses. Jazaei *et al.* (2022) reported that 3 mm polyacrylic fibers at 0.4–0.6% w/w increased WHC, while acrylonitrile butadiene styrene pellets decreased WHC.[48] Wang *et al.* (2023) found that small PE MPs (150 μm, 2% w/w) increased WHC in loamy soil by raising porosity.[49] In addition, Neubert *et al.* (2025) showed that effects of MPs on soil hydraulic properties depended strongly on soil texture.[9] PET microfibers at 0.4% w/w generally increased porosity and air-filled pore volume, whereas PS and PP particles (0.4% w/w) reduced porosity and altered hydraulic conductivity, enhancing water flow in finer soils but clogging pores in sandy soils.[9] In our study, LDPE particles caused the largest increase in soil water content, while PES fibers caused the lowest. These differences likely reflect MP size, shape, and polymer properties, as our LDPE particles were one-tenth the size of those used by Jazaei *et al.* (2022) and Rillig *et al.* (2021).[38,48]

Two distinct pathways could have contributed to the observed responses. Physical pathways include pore bridging or clogging, altered aggregation and bulk density, changes in aeration and water flow, and mechanical effects on root penetration. Chemical pathways include leaching of additives or oligomers, adsorption or desorption of nutrients, and changes in dissolved organic matter.

### Microbiome network responses and functional links to plant performance

Microbial network analysis revealed that LDPE promoted the most substantial increase in rhizosphere microbial co-occurrence complexity, with higher edge density, clustering coefficient, and natural connectivity. Such patterns suggest increased microbial connectivity, potentially due to the surface properties of LDPE, which promote microbial colonization and biofilm formation,[50–53] or even its potential use as a carbon-rich substrate.[54,55] Network centrality was used to identify central candidate ASVs, not ecological keystone taxa, and edges represent covariation rather than interaction. New central candidate ASVs emerged in the LDPE treatment, including *Vicinamibacteraceae* (ASV01049) and *Pseudolabrys* (ASV11937), both potentially linked to plant-associated processes and organic matter degradation.[56,57] The absence of root length reductions in the presence of LDPE suggests that these microbial changes may strengthen locally resilient microbial communities that maintain or even promote functional interactions, possibly through enhanced water retention or by serving as surfaces for microbial colonization and biofilm formation.[50,54] The increased connectivity and emergence of new central candidate ASVs could further support nutrient cycling and potentially buffer environmental stress. The design therefore supports MP-type-specific associations, but it does not isolate polymer-specific mechanisms or causal links among plant traits, nutrient pools, and network topology. Although transformation and zero replacement reduce compositional artifacts, network edges represent correlations among ASVs and not direct ecological interactions.

Importantly, the observed changes in network topology occurred despite the absence of significant differences in alpha diversity. This is not necessarily contradictory, because alpha diversity summarizes the number and relative distribution of

observed ASVs, whereas the network metrics summarize treatment-specific covariance patterns among retained ASVs. Thus, microbial community richness can remain relatively stable while associations among taxa change. Given the five biological replicates per treatment, however, these treatment-specific networks should be considered exploratory and should not be interpreted as evidence of direct microbial interactions.

By contrast, PES and PP reduced network cohesion, with lower node degree, clustering coefficients, and centrality measures. This fragmentation suggests reduced microbial cooperation and stability,[58] consistent with the observed negative effects on root length. Loss of central candidate ASVs could weaken nutrient cycling, pathogen suppression, and other plant-beneficial functions. Network robustness also declined under PES, PP, and PS, although slight increases in vertex and edge connectivity for PP and PS may indicate compensatory adaptations.[59]

PS caused only minor changes in network structure, *e.g.*, slightly increased edge density without major connectivity loss, but altered the identity of candidate central taxa. Gains in influence of nitrifiers, such as *Nitrospira japonica*, likely explain the moderate $NO_3^-$ increase in PS-treated soils, suggesting targeted functional shifts rather than broad community disruption.[40] The limited effect on root and shoot metrics under PS further supports a more functionally resilient microbial community. Since each network was inferred from five biological replicates and correlations may be affected by compositional closure, sparsity, and shifts in treatment-related abundance, the results are interpreted as co-occurrence patterns rather than as direct microbial interactions.

## Conclusions

Our findings demonstrate that MP effects on early wheat growth, nutrient dynamics, and rhizosphere microbial interactions are polymer-specific and interconnected. At 0.4% w/w, PP and PES significantly altered soil properties and reduced root growth. These effects were linked to fragmented microbial networks, loss of central candidate ASVs, and potential suppression of nitrifying activity. In contrast, LDPE enhanced microbial network complexity and soil moisture, suggesting improved microbial integration and possible stress buffering. PS induced only minor structural changes, with subtle shifts favoring nitrification but without major network disruption.

Despite MP-induced changes in soil moisture and $NH_4^+$ concentrations, leaf growth, nutrient uptake, and chlorophyll content remained unaffected, indicating that the early wheat root systems provided sufficient support to the shoots at this developmental stage. Network analyses further revealed that LDPE strengthened microbial connectivity, while PP and PES weakened it, and PS caused only limited reorganization. These results highlight that physicochemical properties of MPs – such as polymer type and shape – govern their impact on plant–soil–microbiome interactions.

Limits of the study are that suppliers' documentation did not declare added plasticizers for the purchased particle materials, and that additives, oligomers, surface oxidation, and leachates were not independently quantified. Therefore, potential chemical effects cannot be separated from physical effects associated with particle size and morphology. Initial rhizosphere responses may be attenuated by resilience, persist, or accumulate during the crop cycle. However, our short-term experiment was unable to distinguish between these possibilities or support direct field extrapolation.

Overall, our study emphasizes the importance of rhizosphere microbiome robustness in mediating plant responses to MP stress. It also underlines the need for future research using dose–response designs with MP concentration gradients, longer growth periods, diverse soil types, and field conditions. Such work is essential to fully understand how MPs influence soil functionality, microbial resilience, and crop productivity.

## Author contributions

K. J. N.: conceptualization, data curation, formal analysis, investigation, methodology, writing: original draft. S. W.: data curation, formal analysis, investigation, methodology, software, writing: original draft. M. S.: funding acquisition, investigation, project administration, resources, supervision, validation, writing: review & editing. N. B.: conceptualization, funding acquisition, investigation, project administration, resources, supervision, validation, writing: review & editing.

## Conflicts of interest

There are no conflicts to declare.

## Data availability

The data supporting this article have been included as part of the supplementary information (SI): Fig. S1 and S2, additional MP characteristics; Fig. S3, stereomicroscopic pictures of winter wheat roots; Fig. S4–S6, additional plant performance data; Fig. S7–S9, additional soil nutrient data; Fig. S10, rarefaction curve of amplicon sequence variants (ASVs); Fig. S11, bacterial community structure; Fig. S12, ASV-level differential-abundance analysis of bacterial community structure; Table S1, relevant assignments of functional groups of PET in Raman spectra; Table S2, parameter set for WinRHIZO analysis; Table S3, two-way ANOVA testing the effect of root zone and MP type; Table S4, statistical analysis of different alpha diversity measures; Tables S5–S8, global network properties of the microbial co-occurrence network. The raw sequence data for processing and statistical analysis of the microbiome, which is not included in the Supplementary Material, is included in the short read archive of National Center for Biotechnology Information (NCBI) under accession number PRJNA1422079. See URL: https://www.ncbi.nlm.nih.gov/sra/?term=PRJNA1422079. Supplementary information is available. See DOI: https://doi.org/10.1039/d6em00205f.

 This journal is © The Royal Society of Chemistry 2026

## Acknowledgements

All authors acknowledge the financial support received from the German Federal Ministry of Research, Technology and Space (BMFTR) for the μPlastic project (grant no.: 031B0907B, 031B0907C), which made this study possible.

## Notes and references

1 S. J. Cusworth, W. J. Davies, M. R. McAinsh, A. S. Gregory, J. Storkey and C. J. Stevens, Agricultural fertilisers contribute substantially to microplastic concentrations in UK soils, *Commun. Earth Environ.*, 2024, **5**(1), 7, DOI: 10.1038/s43247-023-01172-y.

2 M. M. Rana, M. R. Haque, S. S. Tasnim and M. M. Rahman, The potential contribution of microplastic pollution by organic fertilizers in agricultural soils of Bangladesh: quantification, characterization, and risk appraisals, *Front. Environ. Sci.*, 2023, **11**, 1205603, DOI: 10.3389/fenvs.2023.1205603.

3 Y. M. Lozano and M. C. Rillig, Effects of Microplastic Fibers and Drought on Plant Communities, *Environ. Sci. Technol.*, 2020, **54**(10), 6166–6173, DOI: 10.1021/acs.est.0c01051.

4 Y. Liu, M. Xiao, M. Shahbaz, Z. e. Hu, Z. Zhu, S. Lu, Y. Yu, H. Yao, J. Chen and T. Ge, Microplastics in soil can increase nutrient uptake by wheat, *J. Hazard. Mater.*, 2022, **438**, 129547, DOI: 10.1016/j.jhazmat.2022.129547.

5 K. J. Neubert and N. Brüggemann, Soil texture modifies the impact of microplastics on winter wheat growth, *J. Soils Sediments*, 2025, **25**(4), 1340–1357, DOI: 10.1007/s11368-025-04016-8.

6 A. A. de Souza Machado, C. W. Lau, J. Till, W. Kloas, A. Lehmann, R. Becker and M. C. Rillig, Impacts of Microplastics on the Soil Biophysical Environment, *Environ. Sci. Technol.*, 2018, **52**(17), 9656–9665, DOI: 10.1021/acs.est.8b02212.

7 R. Ingraffia, G. Amato, V. Bagarello, F. G. Carollo, D. Giambalvo, M. Iovino, A. Lehmann, M. C. Rillig and A. S. Frenda, Polyester Microplastic Fibers affect Soil Physical Properties and Erosion as a Function of Soil Type, *Soil*, 2021, **2021**, 1–22, DOI: 10.5194/soil-2021-136.

8 R. Ingraffia, G. Amato, M. Iovino, M. C. Rillig, D. Giambalvo and A. S. Frenda, Polyester microplastic fibers in soil increase nitrogen loss via leaching and decrease plant biomass production and N uptake, *Environ. Res. Lett.*, 2022, **17**(5), 054012, DOI: 10.1088/1748-9326/ac652d.

9 K. J. Neubert, L. Weihermüller, H. Vereecken and N. Brüggemann, Soil texture governs the influence of different microplastics on soil hydraulic properties, *Vadose Zone J.*, 2025, **24**(5), e70044, DOI: 10.1002/vzj2.70044.

10 J. Zhou, H. Gui, C. C. Banfield, Y. Wen, H. Zang, M. A. Dippold, A. Charlton and D. L. Jones, The microplastisphere: Biodegradable microplastics addition alters soil microbial community structure and function, *Soil Biol. Biochem.*, 2021, **156**, 108211, DOI: 10.1016/j.soilbio.2021.108211.

11 S. Kublik, S. Gschwendtner, T. Magritsch, V. Radl, M. C. Rillig and M. Schloter, Microplastics in soil induce a new microbial habitat, with consequences for bulk soil microbiomes, *Front. Environ. Sci.*, 2022, **10**, 989267, DOI: 10.3389/fenvs.2022.989267.

12 Y. M. Lozano, J. F. Dueñas, C. Zordick and M. C. Rillig, Microplastic fibres affect soil fungal communities depending on drought conditions with consequences for ecosystem functions, *Environ. Microbiol.*, 2024, **26**(2), e16549, DOI: 10.1111/1462-2920.16549.

13 V. K. Aralappanavar, R. Mukhopadhyay, Y. Yu, J. Liu, A. Bhatnagar, S. M. Praveena, Y. Li, M. Paller, T. M. Adyel, J. Rinklebe, N. S. Bolan and B. Sarkar, Effects of microplastics on soil microorganisms and microbial functions in nutrients and carbon cycling – A review, *Sci. Total Environ.*, 2024, **924**, 171435, DOI: 10.1016/j.scitotenv.2024.171435.

14 Z. Chen, L. J. Carter, S. A. Banwart and P. Kay, Microplastics in Soil–Plant Systems: Current Knowledge, Research Gaps, and Future Directions for Agricultural Sustainability, *Agronomy*, 2025, **15**(7), 1519, DOI: 10.3390/agronomy15071519.

15 H. Xie, *et al.*). Microplastics modify the microbial-mediated carbon metabolism in mangroves, *Environ. Chem. Lett.*, 2024, **22**, 961, DOI: 10.1007/s10311-024-01704-8.

16 Z. Tan, *et al.*). Natural Dynamics: Fresh Insight into the Succession of Microplastic-Borne Bacterial Communities along Riverine Courses to the Ocean, *Environ. Sci. Technol.*, 2025, **59**, 9754, DOI: 10.1021/acs.est.5c00590.

17 L. Lärm, F. M. Bauer, N. Hermes, J. van der Kruk, H. Vereecken, J. Vanderborght, T. H. Nguyen, G. Lopez, S. J. Seidel, F. Ewert, A. Schnepf and A. Klotzsche, Multi-year belowground data of minirhizotron facilities in Selhausen, *Sci. Data*, 2023, **10**(1), 672, DOI: 10.1038/s41597-023-02570-9.

18 B. Peters, G. Blume-Werry, A. Gillert, S. Schwieger, U. F. von Lukas and J. Kreyling, As good as human experts in detecting plant roots in minirhizotron images but efficient and reproducible: the convolutional neural network "RootDetector", *Sci. Rep.*, 2023, **13**(1), 1399, DOI: 10.1038/s41598-023-28400-x.

19 S. Piehl, A. Leibner, M. G. J. Löder, R. Dris, C. Bogner and C. Laforsch, Identification and quantification of macro- and microplastics on an agricultural farmland, *Sci. Rep.*, 2018, **8**(1), 17950, DOI: 10.1038/s41598-018-36172-y.

20 M. C. Rillig, A. Lehmann, A. A. de Souza Machado and G. Yang, Microplastic effects on plants, *New Phytol.*, 2019, **223**(3), 1066–1070, DOI: 10.1111/nph.15794.

21 M. C. Rillig and A. Lehmann, Microplastic in terrestrial ecosystems, *Ecology*, 2020, **368**(6498), 2, DOI: 10.1126/science.abb5979.

22 U. Meier, *Growth Stages of Mono- and Dicotyledonous Plants: BBCH Monograph*, ed. U. Meier, Julius Kühn-Institute, 2 edn, 2018, DOI: 10.5073/20180906-074619.

23 H. K. Lichtenthaler and A. R. Wellburn, Determinations of total carotenoids and chlorophylls a and b of leaf extracts

in different solvents, *Biochem. Soc. Trans.*, 1983, **11**(5), 591–592, DOI: 10.1042/bst0110591.

24 A. Schöler, S. Jacquiod, G. Vestergaard, S. Schulz and M. Schloter, Analysis of soil microbial communities based on amplicon sequencing of marker genes, *Biol. Fertil. Soils*, 2017, **53**(5), 485–489, DOI: 10.1007/s00374-017-1205-1.

25 E. Afgan, D. Baker, M. van den Beek, D. Blankenberg, D. Bouvier, M. Čech, J. Chilton, D. Clements, N. Coraor, C. Eberhard, B. Grüning, A. Guerler, J. Hillman-Jackson, G. Von Kuster, E. Rasche, N. Soranzo, N. Turaga, J. Taylor, A. Nekrutenko and J. Goecks, The Galaxy platform for accessible, reproducible and collaborative biomedical analyses: 2016 update, *Nucleic Acids Res.*, 2016, **44**(W1), W3–W10, DOI: 10.1093/nar/gkw343.

26 M. Martin, Cutadapt removes adapter sequences from high-throughput sequencing reads, *EMBnet J.*, 2011, 10–12, DOI: 10.14806/ej.17.1.200.

27 S. Andrews, *FastQC: A Quality Control Tool for High Throughput Sequence Data*, 2010, https://www.bioinformatics.babraham.ac.uk/projects/fastqc/.

28 B. J. Callahan, P. J. McMurdie, M. J. Rosen, A. W. Han, A. J. A. Johnson and S. P. Holmes, DADA2: High-resolution sample inference from Illumina amplicon data, *Nat. Methods*, 2016, **13**, 581–583, DOI: 10.1038/nmeth.3869.

29 C. Quast, E. Pruesse, P. Yilmaz, J. Gerken, T. Schweer, P. Yarza, J. Peplies and F. O. Glöckner, The SILVA ribosomal RNA gene database project: Improved data processing and web-based tools, *Nucleic Acids Res.*, 2013, **41**(D1), D590–D596, DOI: 10.1093/nar/gks1219.

30 R Core Team, *R: A language and environment for statistical computing*, R Foundation for Statistical Computing, 2023, Vienna, Austria, https://www.R-project.org/.

31 J. C. Oliveros, Venny. An interactive tool for comparing lists with Venn's diagrams, 2007, https://bioinfogp.cnb.csic.es/tools/venny/index.html.

32 S. Peschel, C. L. Müller, E. Von Mutius, A. L. Boulesteix and M. Depner, Network construction and comparison for microbiome data in R, in *Briefings in Bioinformatics*, Oxford University Press, 2021, vol. 22, 4, DOI: 10.1093/bib/bbaa290.

33 Y. Lian, R. Shi, J. Liu, A. Zeb, Q. Wang, J. Wang, M. Yu, J. Li, Z. Zheng, N. Ali, Y. Bao and W. Liu, Effects of polystyrene, polyethylene, and polypropylene microplastics on the soil-rhizosphere-plant system: Phytotoxicity, enzyme activity, and microbial community, *J. Hazard. Mater.*, 2024, **465**, 133417, DOI: 10.1016/j.jhazmat.2023.133417.

34 D. J. Hernandez, A. S. David, E. S. Menges, C. A. Searcy and M. E. Afkhami, Environmental stress destabilizes microbial networks, *ISME J.*, 2021, **15**(6), 1722–1734, DOI: 10.1038/s41396-020-00882-x.

35 R. Huang, S. P. McGrath, P. R. Hirsch, I. M. Clark, J. Storkey, L. Wu, J. Zhou and Y. Liang, Plant–microbe networks in soil are weakened by century-long use of inorganic fertilizers, *Microb. Biotechnol.*, 2019, **12**(6), 1464–1475, DOI: 10.1111/1751-7915.13487.

36 H. Li and L. Liu, Short-term effects of polyethene and polypropylene microplastics on soil phosphorus and nitrogen availability, *Chemosphere*, 2022, **291**(Pt 2), 132984, DOI: 10.1016/j.chemosphere.2021.132984.

37 O. E. Ayiti and O. O. Babalola, Factors Influencing Soil Nitrification Process and the Effect on Environment and Health, *Front. Sustain. Food Syst.*, 2022, **6**, 821994, DOI: 10.3389/fsufs.2022.821994.

38 M. C. Rillig, M. Hoffmann, A. Lehmann, Y. Liang, M. Lück and J. Augustin, Microplastic fibers affect dynamics and intensity of CO2 and N2O fluxes from soil differently, *Microplast. Nanoplast.*, 2021, **1**(1), 3, DOI: 10.1186/s43591-021-00004-0.

39 A. A. de Souza Machado, C. W. Lau, W. Kloas, J. Bergmann, J. B. Bachelier, E. Faltin, R. Becker, A. S. Görlich and M. C. Rillig, Microplastics Can Change Soil Properties and Affect Plant Performance, *Environ. Sci. Technol.*, 2019, **53**(10), 6044–6052, DOI: 10.1021/acs.est.9b01339.

40 J. Lee, S. Jeong, C. Long and K. Chandran, Size dependent impacts of a model microplastic on nitrification induced by interaction with nitrifying bacteria, *J. Hazard. Mater.*, 2022, **424**, 127363, DOI: 10.1016/j.jhazmat.2021.127363.

41 W. Römer, J. Augustin and G. Schilling, The relationship between phosphate absorption and root length in nine wheat cultivars, *Plant Soil*, 1988, **111**, 199–201, DOI: 10.1007/BF02139938.

42 S. AđAlsteinsson, J. K. Schjørring and P. Jensen, Regulation of Phosphate Influx in Winter Wheat: Root-Shoot Phosphorus Interactions, *J. Plant Physiol.*, 1994, **143**(6), 681–686, DOI: 10.1016/S0176-1617(11)81157-0.

43 L. Erdei, Z. Oláh and A. Bérczi, Nutrition of winter wheat during the life cycle. II. Influx and translocation of potassium and phosphorus, *Physiol. Plant.*, 2006, **58**, 131–135, DOI: 10.1111/j.1399-3054.1983.tb04155.x.

44 S. Yan, S. Zhang, B. Xu, P. Yan, J. Wang, H. Wang and M. Aurangzeib, Microplastics change the leaching of nitrogen and potassium in Mollisols, *Sci. Total Environ.*, 2023, **878**, 163121, DOI: 10.1016/j.scitotenv.2023.163121.

45 T. Jin, X. Liu, J. Cui, J. Peng and Q. Liu, Macroplastics Quantity and Its Influence on Soil Nutrients in Typical Plastic Film Mulching Farmland in Northern Xinjiang, *Agriculture*, 2024, **14**(5), 734, DOI: 10.3390/agriculture14050734.

46 T. Zhao, Y. M. Lozano and M. C. Rillig, Microplastics Increase Soil pH and Decrease Microbial Activities as a Function of Microplastic Shape, Polymer Type, and Exposure Time, *Front. Environ. Sci.*, 2021, **9**, 675803, DOI: 10.3389/fenvs.2021.675803.

47 X. Yin, C. F. Seavert, J. Turner, R. Núñez-Elisea and H. Cahn, Effects of Polypropylene Groundcover on Soil Nutrient Availability, Sweet Cherry Nutrition, and Cash Costs and Returns, *HortScience*, 2007, **42**(1), 147–151, DOI: 10.21273/HORTSCI.42.1.147.

48 F. Jazaei, T. J. Chy and M. Salehi, Can Microplastic Pollution Change Soil-Water Dynamics? Results from Controlled Laboratory Experiments, *Water*, 2022, **14**(21), 3430, DOI: 10.3390/w14213430.

49 Z. Wang, W. Li, W. Li, W. Yang and S. Jing, Effects of microplastics on the water characteristic curve of soils with

 This journal is © The Royal Society of Chemistry 2026

different textures, *Chemosphere*, 2023, **317**, 137762, DOI: 10.1016/j.chemosphere.2023.137762.
50 Y. Huang, Y. Zhao, J. Wang, M. Zhang, W. Jia and X. Qin, LDPE microplastic films alter microbial community composition and enzymatic activities in soil, *Environ. Pollut.*, 2019, **254**, 112983, DOI: 10.1016/j.envpol.2019.112983.
51 C. Li, Q. Cui, Y. Li, K. Zhang, X. Lu and Y. Zhang, Effect of LDPE and biodegradable PBAT primary microplastics on bacterial community after four months of soil incubation, *J. Hazard. Mater.*, 2022, **429**, 128353, DOI: 10.1016/j.jhazmat.2022.128353.
52 L. Rong, L. Zhao, L. Zhao, Z. Cheng, Y. Yao, C. Yuan, L. Wang and H. Sun, LDPE microplastics affect soil microbial communities and nitrogen cycling, *Sci. Total Environ.*, 2021, **773**, 145640, DOI: 10.1016/j.scitotenv.2021.145640.
53 H. Ya, Y. Xing, T. Zhang, M. Lv and B. Jiang, LDPE microplastics affect soil microbial community and form a unique plastisphere on microplastics, *Appl. Soil Ecol.*, 2022, **180**, 104623, DOI: 10.1016/j.apsoil.2022.104623.
54 M. Gong, G. Yang, L. Zhuang and E. Y. Zeng, Microbial biofilm formation and community structure on low-density polyethylene microparticles in lake water microcosms, *Environ. Pollut.*, 2019, **252**, 94–102, DOI: 10.1016/j.envpol.2019.05.090.
55 Y. Chen, X. Wang, X. Wang, T. Cheng, K. Fu, Z. Qin and K. Feng, Biofilm Structural and Functional Features on Microplastic Surfaces in Greenhouse Agricultural Soil, *Sustainability*, 2022, **14**(12), 7024, DOI: 10.3390/su14127024.
56 O. S. Gonçalves, A. S. Fernandes, S. M. Tupy, T. G. Ferreira, L. N. Almeida, C. J. Creevey and M. F. Santana, Insights into plant interactions and the biogeochemical role of the globally widespread Acidobacteriota phylum, *Soil Biol. Biochem.*, 2024, **192**, 109369, DOI: 10.1016/j.soilbio.2024.109369.
57 N. Arunrat, T. Uttarotai, P. Kongsurakan, S. Sereenonchai and R. Hatano, Bacterial Community Structure in Soils with Fire-Deposited Charcoal Under Rotational Shifting Cultivation of Upland Rice in Northern Thailand, *Ecol. Evol.*, 2025, **15**(2), e70851, DOI: 10.1002/ece3.70851.
58 B. S. Griffiths and L. Philippot, Insights into the resistance and resilience of the soil microbial community, *FEMS Microbiol. Rev.*, 2013, **37**(2), 112–129, DOI: 10.1111/j.1574-6976.2012.00343.x.
59 D. Berry and S. Widder, Deciphering microbial interactions and detecting keystone species with co-occurrence networks, *Front. Microbiol.*, 2014, **5**, 219, DOI: 10.3389/fmicb.2014.00219.